The Relationship between Cold-Frontal Radar Echoes and Selected Surface Kinematic Parameters

RICHARD D. THOMAS, JR.[1]

Systems Development Office, National Weather Service, NOAA, Silver Spring, MD 20910

DAVID D. HOUGHTON

Department of Meteorology, University of Wisconsin, Madison 53706

(Manuscript received 1 February 1979, in final form 10 August 1979)

ABSTRACT

This study examines the relationship between the radar echo parameters of area coverage and intensity, and the surface kinematic fields of divergence, divergence of moisture flux and relative vorticity. The study was limited to 11 cold frontal cases during the period March 1976–March 1977, and involved 99 echoes. Fine-resolution digitized radar data were used from two midwestern and one eastern United States sites. The data were analyzed on a computer-interactive video system. The area coverage did not correlate significantly with any of the surface parameters tested. However, the intensity parameters did show significant relationships with the surface parameters, the best being with relative vorticity. The correlations were higher when surface data from 1 h before the time of the echo were used, with coefficients as high as 0.5.

1. Introduction

The forecasting of precipitation always has been an important aspect of operational weather forecasting. In recent years, much work has been done toward producing more accurate and more automated short-range local precipitation forecasts.

A problem in any objective mesoscale forecasting is that of getting observational data on a small enough scale. Surface observing stations are generally ~100 km apart, and upper air observing stations are 300–400 km apart. On the other hand, radar and satellite data are of a continuous nature, in both time and space. The use of radar in precipitation forecasting is the motivation behind this investigation.

In order to use radar as an objective tool in precipitation forecasting, procedures must be developed to forecast echo movement and changes with time. Several extrapolation techniques have been developed which give favorable results (see Elvander, 1976). However, these forecasts probably could be improved by using relationships with other atmospheric variables in addition to the extrapolation techniques. First, however, these relationships must be better understood.

The objective of this analysis was to examine the relationships between radar parameters (such as area coverage, growth, intensity and the change of these parameters in time) and surface kinematic fields [such as divergence, divergence of moisture (mixing ratio) and relative vorticity]. These kinematic fields were expected to have a direct relationship with precipitation. Surface data were preferred over upper air data because of greater abundance in time and space.

Numerous studies in the past have successfully related the echo movement to upper level winds, particularly the 700 mb level (see Harper and Beimers, 1958; Boucher and Wexler, 1961; Newton and Fankhauser, 1964; Cruz, 1973; Mielke and Houghton, 1977). Far less has been done concerning relationships with the surface variables, particularly relationships between subsynoptic-scale data and the detailed features of individual radar echoes. To limit the scope of this study, only cold frontal echoes were used.

2. Past work

Byers and Braham (1949) reported that during the Thunderstorm Project, weak convergence was present during the early cumulus stage of thunderstorm development. This was 20–30 min before the radar detected the storm. However, when older storms were in the area, their outflow dominated the sur-

[1] Research was carried out while author was on a fellowship program at the Department of Meteorology, University of Wisconsin at Madison.

0027-0644/79/121589-11$06.75

TABLE 1. Characteristics of WSR-57.[1]

Wavelength	10.3 cm
Transmitted frequency	1250 mHz
Beam width	2°
Range	125 n mi
Pulse repetition frequency	164 pps
Width of pulse	4 s
Peak transmitted power	410 kW
Scan rate	3 rpm
Antenna gain	38 dB
Standard antenna elevation	0.5°

[1] Information received by personal communication with Jim Schaeffer, Office of Technical Services, National Weather Service, June 1978.

face wind. This made it impossible to find areas of inflow near new storms.

Austin and Blackmer (1956) studied the precipitation patterns of 30 summertime cold fronts in Massachusetts using radar data. Synoptic-scale parameters such as the 700 mb temperature contrast across the front, warm air static stabilities and 850 mb dew-point spread were correlated to the area covered by precipitation. The correlation coefficients were generally poor, ranging from 0.0 to 0.4. In a similar study with wintertime cold-frontal precipitation, Cox (1959) found that out of seven synoptic-scale parameters, only an instability index correlated significantly with total radar-scope coverage. Twenty-one cold-frontal situations were used for that study.

In another study, Myers (1964) studied the role of the synoptic situation and local topography on the pattern of showers in central Pennsylvania. In comparing several synoptic variables with the amount of radar scope coverage, the surface dew-point depression produced the highest significant correlation coefficient. The synoptic parameters were also compared with various "scope scatter" coefficients. Again dew-point depression showed the best relationship.

TABLE 2. Comparison of rainfall rates with radar power returned and D/RADEX levels (by Saffle, 1976). All numbers are range correlated.*

Rainfall rate (mm h^{-1})	LogZ	Threshold levels (D/RADEX)
0.508	1.83	1
1.27	2.47	2
2.54	2.93	3
5.08	3.43	4
12.7	4.07	5
25.4	4.55	6
50.8	5.03	7
127.0	5.67	8
254.0	6.15	9

* The D/RADEX rainfall rates were changed after this research was completed (see Saffle and Greene, 1978).

Using data from two experiments carried out in the summers of 1971 and 1973 in southern Florida, Ulanski and Garstang (1978) studied the role of surface divergence and relative vorticity in convective precipitation. Data from a dense observing network, part of the Florida Area Cumulus Experiment, was used to study about 50 storms. It was shown by using a "spatial index" that the maximum point rainfall in a storm is directly proportional to the surface convergence gradient and size of the convergence area. The size of the convergence area was also found to be one of the most important factors in determining the total rainfall produced by individual storms. Using data from the same Florida experiment, Pielke and Cotton (1977) also related mesoscale kinematic features to rainfall events.

3. Data sources and facilities used

The radar data for this study came from three National Weather Service sites (Pittsburgh, Pennsylvania; Kansas City, Missouri; and Monett, Missouri). These sites are part of the Digitized Radar Experiment (D/RADEX), which was established in late 1971 and early 1972. Basically, each site consists of a WSR-57 (Weather Surveillance Radar-57) interfaced to a NOVA 1200 minicomputer. Additional information concerning D/RADEX can be found in a paper by McGrew (1972). Table 1 summarizes the radar's characteristics. The fundamental resolution is 1 n mi in the radial direction and 2° in the azimuthal direction. The data for a complete radar scope image is archived every 12 min. Each 2° by 1 n mi data bin has a value in the range 0–9 (D/RADEX levels). Table 2 compares the rainfall rates with radar power returned and D/RADEX levels.

The Man-computer Interactive Data Access System (McIDAS), developed by the Space Science and Engineering Center at the University of Wisconsin-Madison, was used for the processing of the radar data. A complete description of the system is given by Smith (1975) and Chatters and Suomi (1975). The system consists of a Datacraft 6024/5 computer, digital disks and I/O devices, interfaced to a color monitor and CRT display by a video display system. An applications program was used to give a frequency distribution of the intensity level of each pixel in an enclosed area. This was used to generate values of area coverage and intensity for each echo.

Hourly airways surface observations were obtained from the archive of the National Severe Storms Forecast Center in Kansas City. The observations used covered the surface grid areas which were slightly larger than the radar coverage areas. Of these observations, there were actually 24 within the Pittsburgh, 14 within the Kansas City and 11 within the Monett radar coverage area.

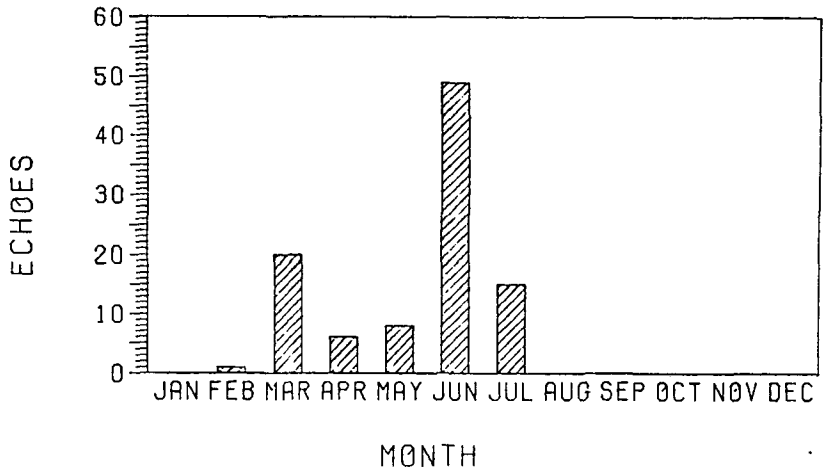

FIG. 1. Number of echoes per month (1976 and 1977 data combined).

4. Methods of analysis of the data

The frontal cases used in this study were generally well defined cold fronts, where the respective radar sites were at least 500 km south of the intersection with the warm front. Quasi-stationary fronts were not used, nor fronts with evidence of a wave near the radar site. Due to logistical and technical difficulties, data were only available for 11 cases of the 30 identified. All cases were between March 1976 and March 1977.

The radar observations used from each of the 11 cases had to meet the criteria that they had at least one (preferably more) distinct echoes which showed somewhat consistent motion and shape. The echoes had to be observed on three consecutive observations, centered on the beginning of an hour. The echoes also had to be completely enclosed by the radar area at all three times. The number of hours of data used from each case varied with the amount of echoes which met the above criteria. Whenever possible, consecutive hours were not used. There was a total of 39 h of observations (three observations used per hour) used from the 11 cases, equally distributed among the three radar sites. From this data set, 99 echoes were studied. Fig. 1 presents a distribution of the number of echoes per month. It is quite clear that the data sampling is strongly biased toward the spring and summer seasons. The average area of the echoes in this study was 1781 km^2, with half of the echoes having an area <750 km^2.

The D/RADEX data were converted to a McIDAS compatible format, giving a display of a 1 n mi $\times$ 1 n mi Cartesian grid in grey scale form. The grid points were given the value of the D/RADEX data bin in which the points fell. Only D/RADEX levels 2 and above were displayed to give better echo definition.

With each set of radar observations, centered on the hour, a frequency distribution of radar return levels was measured for each echo at the three times. These three values were averaged to give values of area coverage, maximum intensity and average rainfall rate for the echo. The rainfall rate as given by the relationship in Table 2 was used to estimate average intensity across the echo area. This was done to avoid the logarithmic scaling of radar intensity. For the purposes of this study, the values were not meant to estimate actual rainfall rates. In cases where there was an increase or decrease through the 24 min period, the magnitude of the change was calculated for that period. This was done by subtracting the value 12 min before from that 12 min after the hour. In cases where the trends in the first and second halves of the period were not consistent, the change was ignored. A summary of the means and standard deviations of these parameters is presented as Table 3.

Each of the echoes were classified in five ways: position with respect to the front, relationship with respect to other echoes (in a line, isolated or embedded in a larger area of lighter precipitation), shape (banded or nonbanded), area coverage and geographic location. Table 4 shows the number of echoes in each category.

The classification with respect to frontal position consisted of determining whether the echo was prefrontal, frontal or postfrontal. Frontal echoes in this study are defined as being within 15 n mi of the front.

The second set of classifications was with respect to the type of arrangement the echo was in with other echoes. A line of echoes is defined as several mesoscale areas of precipitation, forming an elongated area of length to width ratio $\geq$ 5:1. Any echo which followed the above definition, or was part of such a feature, was classified as line. If the echo was not part of a line, and was not attached to any other echoes, it was classified as isolated. Echoes which were not part of lines, but were embedded in a larger area of lighter precipitation (D/RADEX level

TABLE 3. Summary of the radar echo statistics.

Equivalent radius (km)	
Average	23.8
Median	15.5
Area coverage (km^2)	
Average	1781
Standard deviation	3083
Minimum	54
Maximum	17811
Change of area coverage [km^2(24 min)$^{-1}$]	
Average	−0.3
Standard deviation	1033
Maximum intensity (D/RADEX levels)	
Average	4.1
Standard deviation	1.5
Change of maximum intensity [D/RADEX levels(24 min)$^{-1}$]	
Average	+0.06
Standard deviation	0.8
Average rainfall rate (mm h^{-1})	
Average	2.54
Standard deviation	2.55
Change of rainfall rates [mm h^{-1}(24 min)$^{-1}$]	
Average	+0.29
Standard deviation	1.4

1) were classified conglomerate. These echoes were sometimes quite close to other mesoscale areas in the same general pattern.

The third classification was simply whether the echo was banded or not. A banded echo is defined here as having a length to width ratio of at least 2:1, as opposed to the greater ratio associated with lines of echoes. Banded echoes may or may not be echoes which are part of lines.

The area coverage classification consisted of separating the larger (>750 km^2) and smaller echoes (<750 km^2). The breakpoint of 750 km^2 was chosen because it split the total sample in half.

The geographic classification simply separated the Pittsburgh radar site echoes from the two Midwestern radar site echoes.

TABLE 4. Number of echoes in each classification.

Category	Number of echoes
All	99
Midwest	65
Pittsburgh	34
Prefrontal	62
Frontal	21
Postfrontal	16
Line	43
Isolated	31
Conglomerate	25
Banded	54
Nonbanded	45
Large area	50
Small area	49

The values of surface divergence, divergence of moisture flux and relative vorticity were calculated for a 0.5° 18 by 18 latitude/longitude grid. There were separate grids for the midwestern and Pittsburgh sites. The fields were based on the u and v wind components, using simple, centered finite-difference techniques. The u and v grid-point values were calculated using a modified Cressman weighted interpolation scheme (Whittaker, 1976). This method included no special smoothing techniques. The divergence of moisture flux was calculated by multiplying the grid-point values of u and v by the mixing ratio. As an example, Figs. 2, 3 and 4 present analyses of these kinematic fields for one of the radar echo cases. The scale of the features are typical of most cases.

Using an equally spaced distribution of points throughout the echoes, values of the surface parameters were interpolated from grid-point data using an overlapping polynomial technique (Whittaker and Petersen, 1977). The point values were then averaged to give a value for the echo area. The mean values and standard deviations for the surface parameters in the echo areas are presented in Table 5.

The above procedures were repeated with surface data 1 h before the time of the echo. Thus, the echo parameters were compared to values of surface divergence and vorticity 1 h before the echo moved into that area. Values were also calculated for the surface parameters in the echo relative to the mean for the whole grid. The average grid-point

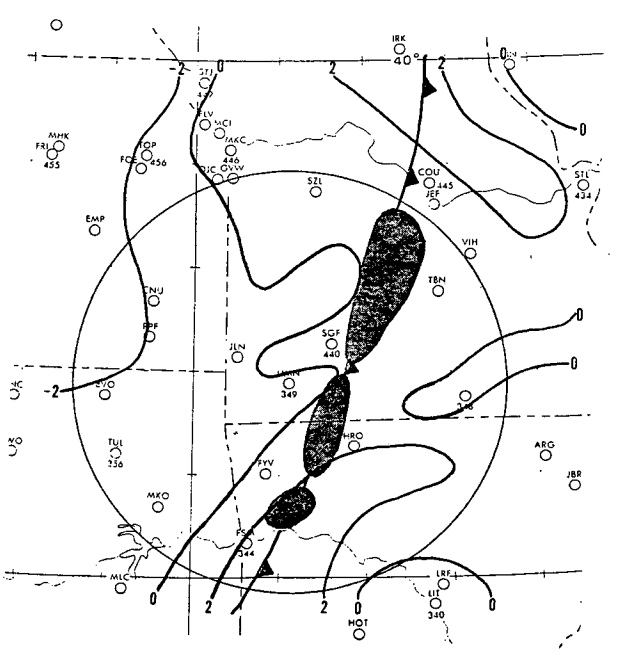

FIG. 2. Surface divergence (10^{-5} s^{-1}) analysis, 1500 GMT 18 April 1976, for the Monett, Missouri radar area. (Shaded areas denote radar echoes.)

value was subtracted from the value of the surface parameter associated with the echo.

5. Relationship of echo parameters with surface kinematic fields

When the various echo parameters were compared with the surface kinematic fields, only a few of the echo parameters gave significant results. The echo parameters of maximum intensity, average rainfall rate and change of average rainfall rate correlated with many of the surface fields used. The area coverage, change of area coverage and change of maximum intensity did not correlate with any surface parameters using the total sample. However, there were a few marginally significant correlations using the echo categories discussed in the previous section. Several categories of echoes did not show any significant correlations at all. These included the Pittsburgh echoes (except for one marginally significant correlation) and the prefrontal, frontal and conglomerate echo categories.

In the following subsections, correlation statistics involving each of the three echo parameters which showed significant results will be discussed. The statistics applying to the total sample will be presented in detail. Only the more important points with the individual categories of echoes will be discussed.

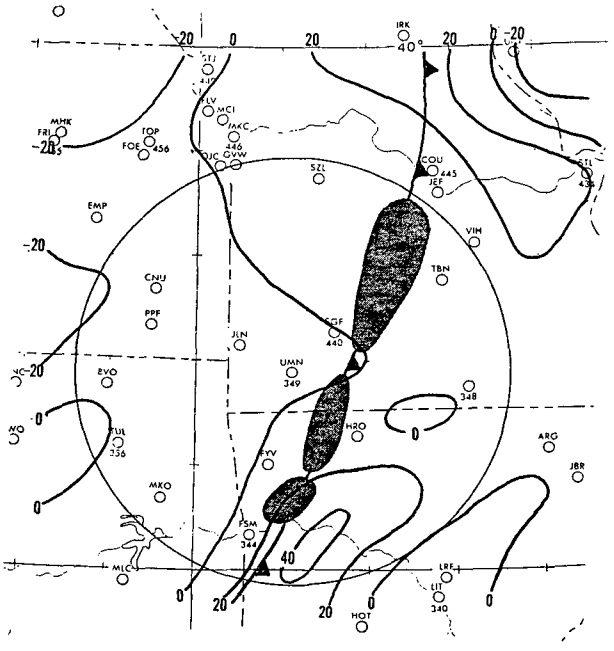

FIG. 3. Surface divergence of moisture flux (10^{-5} s^{-1}) analysis, 1500 GMT 18 April 1976, for the Monett, Missouri radar area. (Shaded areas denote radar echoes.)

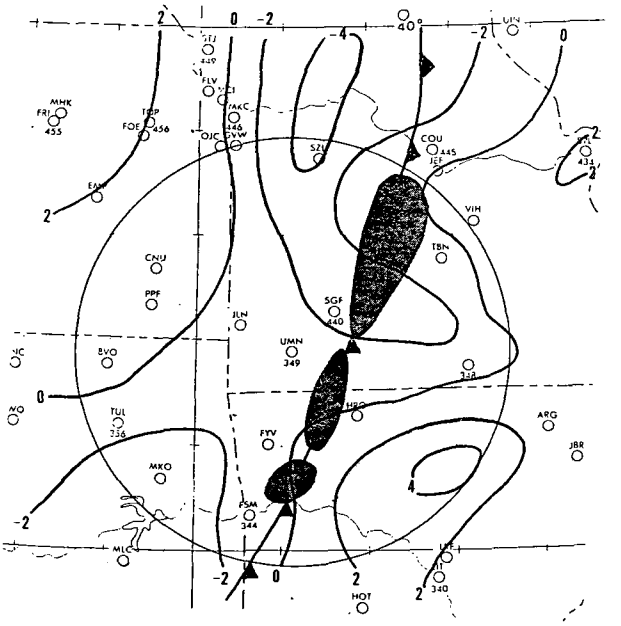

FIG. 4. Surface relative vorticity (10^{-5} s^{-1}) analysis, 1500 GMT 18 April 1976, for the Monett, Missouri radar area. (Shaded areas denote radar echoes.)

a. Maximum intensity

Table 6 shows the correlation coefficients and regression equations for the relationships involving maximum intensity. Relative vorticity gave better

TABLE 5. Summary of surface parameters.

Surface parameter	Mean (10^{-5} s^{-1})	Standard deviation (10^{-5} s^{-1})
Divergence	−0.47	2.40
One hour earlier	−0.66	2.73
Change in 1 h	0.19	2.03
Relative to the grid average	−0.29	2.29
One hour earlier, relative to the grid average	−0.49	2.68
Change in 1 h relative to the grid average	0.20	2.00
Divergence of moisture flux	−7.13	28.80
One hour earlier	−8.95	33.52
Change in 1 h	1.82	24.71
Relative to the grid average	−5.46	27.56
One hour earlier, relative to the grid average	−7.52	33.08
Change in 1 h, relative to the grid average	2.05	24.28
Relative vorticity	0.87	2.36
One hour earlier	0.70	2.59
Change in 1 h	0.17	1.76
Relative to the grid average	0.72	2.24
One hour earlier, relative to the grid average	0.56	2.50
Change in 1 h, relative to the grid average	0.16	1.76

TABLE 6. Correlation coefficients and linear regression equations for the maximum intensity and various surface parameters, ranked in order of highest correlation coefficients. (The critical coefficient magnitude for significance at the 95% confidence interval is 0.23.)

Surface parameter	Linear regression equation*	Correlation coefficient
Relative vorticity, 1 h earlier relative to the grid average	Max Int = 4.04 + 0.24 (Vort)	0.40
Relative vorticity, relative to the grid	Max Int = 3.90 + 0.27 (Vort)	0.40
Divergence of moisture flux, 1 h earlier relative to the grid average	Max Int = 4.05 − 0.02 (DivMF)	−0.38
Relative vorticity, 1 h earlier	Max Int = 4.04 + 0.2 (Vort)	0.35
Relative vorticity	Max Int = 3.89 + 0.22 (Vort)	0.34
Divergence of moisture flux, 1 h earlier	Max Int = 4.04 − 0.015 (DivMF)	−0.34
Divergence, 1 h earlier, relative to the grid average	Max Int = 4.09 − 0.18 (Div)	−0.33
Divergence, 1 h earlier	Max Int = 4.08 − 0.15 (Div)	−0.27
Divergence of moisture flux, relative to the grid average	Max Int = 4.04 − 0.16 (DivMF)	−0.24

* Max Int is the D/RADEX level; the units of Vort, Div and DivMF are 10^{-5} s^{-1}.

correlations than any of the divergence fields, with coefficients as high as 0.4. The correlations were improved slightly by using the values relative to the grid average and values from 1 h earlier than the time the radar echo was observed. In addition, the divergence of moisture flux correlated better than the divergence of the wind field alone.

The relative vorticity gave positive correlations with the maximum intensity, while the divergence parameters correlated negatively. This means that the stronger the relative vorticity is in the area to which an echo is moving, or is already located, the higher the maximum intensity associated with the echo. The negative correlation with the divergence is similar in that the more intense echoes will have had stronger convergence in the same area an hour earlier.

A scatter diagram is presented as Fig. 5, showing the relationship of the relative vorticity 1 h earlier than the echo time, relative to the grid average, to the maximum intensity. The distribution of points seems to be better described by a nonlinear relationship than the least-squares regression line. Fig. 6 shows the distribution of correlation coefficients for the same relationship of Fig. 5, for each of the categories showing significant correlations. The most statistically significant categories to be noted are the banded and larger area categories. Both of these categories had much higher correlations than their counterparts, namely, the nonbanded category, which showed no significant correlations, and the smaller area category.

The banded echoes gave the highest correlation coefficients of any of the echo categories except for the very limited sample of postfrontal echoes. The coefficients which were significant with the surface parameters ranged in absolute value from 0.34 to 0.58. The nonbanded echoes had much lower correlation coefficients, with the maximum intensity of echoes in that category not correlating significantly with any surface parameters.

In general, the correlation coefficients for the

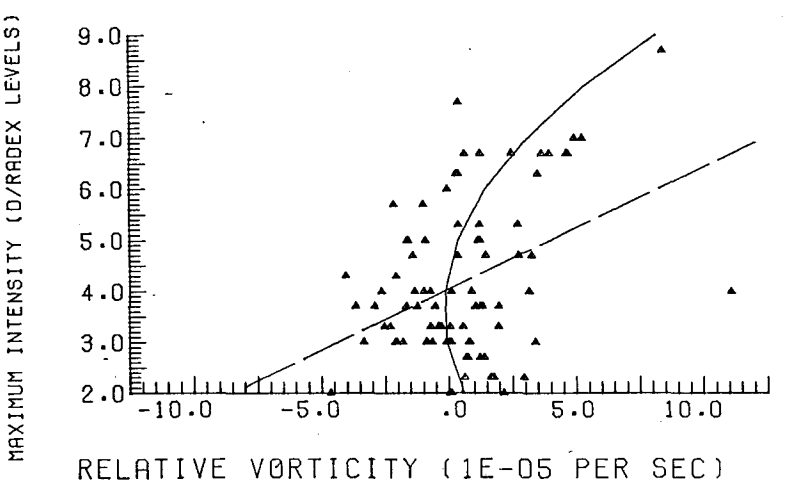

FIG. 5. Scatter diagram of maximum intensity versus the relative vorticity 1 h earlier than the echo, relative to the average grid value of vorticity.

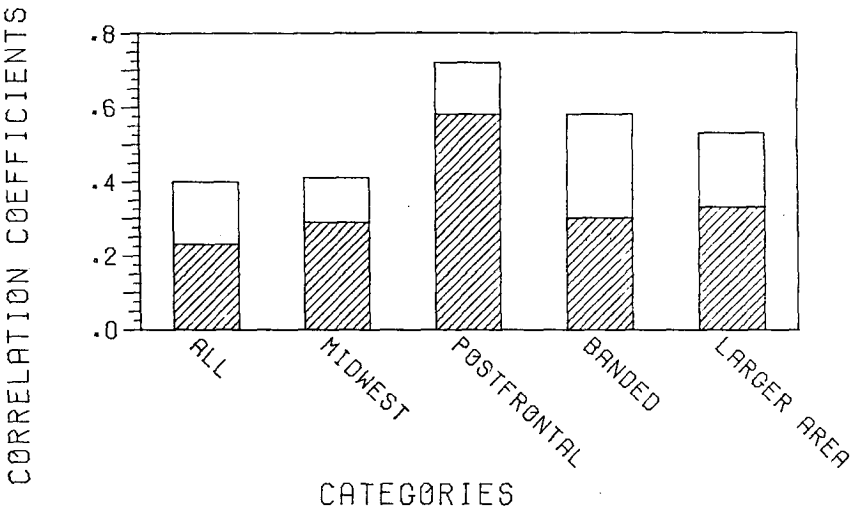

FIG. 6. Distribution of the correlation coefficients for the relationship shown in Fig. 5 by echo category. (Shaded areas denote values which the correlation coefficients must exceed to be significant at the 95% level.)

larger (>750 km^2) echoes were more than twice those of the small echoes, each having the same sample size. The coefficients which were significant with the surface parameters ranged in absolute value from 0.33 to 0.56. Interestingly, the few cases in which the maximum intensity did correlate significantly to a surface parameter for the smaller echoes were cases in which the larger echoes correlated exceptionally poorly. These were the change of divergence of moisture flux during the past hour, and that change relative to the average grid value. The correlation coefficients for these relationships were marginally significant, and had values of 0.39 and 0.38, respectively.

The reason for many of the correlation coefficients with the midwestern echoes being significant, compared with none for the Pittsburgh echoes, is not understood. This may be due solely to the small sample size there, or to some orographic effects. Similar questions arise when trying to explain why the postfrontal echoes correlated significantly, but not the frontal or prefrontal. All of the postfrontal echoes were observed in the midwest sites. These same problems also arise with the other echo parameters to be discussed.

b. Average rainfall rate (radar estimated)

The average rainfall rates of the echoes showed the best correlation to surface parameters of any of the echo parameters tested. The correlations, as shown in Table 7, are similar to those of the maxi-

TABLE 7. Correlation coefficients and linear regression equations for the average rainfall rate and various surface parameters, ranked in order of highest correlation coefficients. (Critical correlation magnitude for significance at the 95% confidence interval is 0.23.)

Surface parameter	Linear regression equation*	Correlation coefficient
Relative vorticity, 1 h earlier, relative to the grid average	ARR = 2.38 + 0.58 (Vort)	0.53
Relative vorticity, 1 h earlier	ARR = 2.34 + 0.52 (Vort)	0.50
Relative vorticity, relative to the grid average	ARR = 2.23 + 0.56 (Vort)	0.47
Divergence of moisture flux, 1 h earlier relative to the grid average	ARR = 2.44 − 0.035 (DivMF)	−0.43
Relative vorticity	ARR = 2.19 + 0.48 (Vort)	0.42
Divergence of moisture flux, 1 h earlier	ARR = 2.41 − 0.03 (DivMF)	−0.40
Divergence, 1 h earlier, relative to the grid average	ARR = 2.5 − 0.39 (Div)	−0.39
Divergence, 1 h earlier	ARR = 2.47 − 0.35 (Div)	−0.35
Change of divergence of moisture flux	ARR = 2.64 + 0.04 (DivMF)	0.34
Change of divergence	ARR = 2.62 + 0.45 (Div)	0.33
Change of divergence of moisture flux, relative to the grid average	ARR = 2.63 + 0.04 (DivMF)	0.33
Change of divergence, relative to the grid average	ARR = 2.62 + 0.43 (Div)	0.32
Divergence of moisture flux, relative to the grid average	ARR = 2.47 − 0.02 (DivMF)	−0.25

Units of average rainfall rate (ARR) are mm h^{-1}, those of Vort, Div and DivMF 10^{-5} s^{-1}.

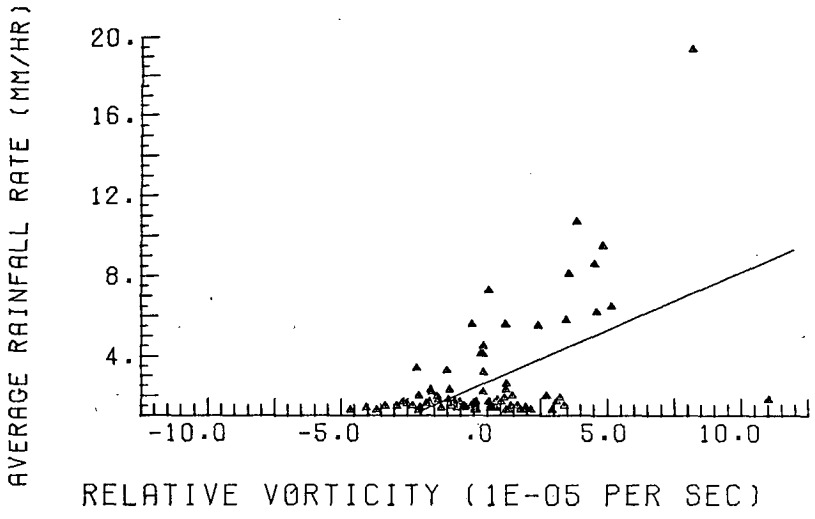

FIG. 7. Scatter diagram of average rainfall rate versus the relative vorticity 1 h earlier than the echo, relative to the average grid value of vorticity.

mum intensity in that the relative vorticity showed the best relationship among all of the surface parameters. Stronger positive vorticity is associated with higher average rainfall rates. The divergence parameters correlated negatively except for the change of divergence which had a positive correlation. These relationships are all consistent with the idea that higher average rainfall rates are associated with stronger convergence in the area to which the echo is moving. As the echo moves into the area, the wind field becomes more divergent at the surface, accounting for the positive change of divergence over the hour. It is interesting to note, though, that the divergence of the wind field alone did not show significant correlation with either the maximum intensity or the average rainfall rate.

A scatter diagram for relative vorticity, 1 h earlier than the echo time and relative to the grid average, versus the average rainfall rate is given in Fig. 7. The plot shows that a wide range of surface vorticities are associated with echoes which have low average rainfall rates. The relationship becomes more organized as the average rainfall rate increases. Fig. 8 shows much the same type of distribution of correlation coefficients among the echo categories as did Fig. 6 with maximum intensity.

As before, the banded and larger echoes showed much better correlation with surface parameters than the nonbanded and smaller echoes. The nonbanded echoes did show marginally significant correlation with the relative vorticity at the same time as the echo, and the same relative to the grid aver-

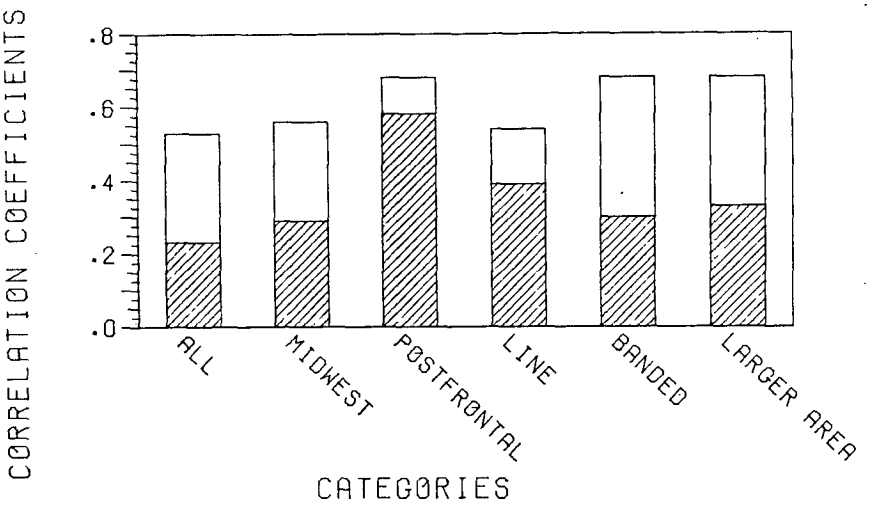

FIG. 8. Distribution of correlation coefficients for the relationship shown in Fig. 7, by echo category. See Fig. 6.

TABLE 8. Correlation coefficients and linear regression equations for the change of average rainfall rate and various surface parameters, ranked in order of highest correlation coefficients. (Critical correlation value for significance at the 95% confidence interval is 0.24.)

Surface parameter	Linear regression equation*	Correlation coefficient
Change of divergence of moisture flux	ΔARR = 0.33 + 0.03 (DivMF)	0.42
Change of divergence of moisture flux, relative to the grid average	ΔARR = 0.32 + 0.03 (DivMF)	0.41
Change of divergence	ΔARR = 0.31 + 0.29 (Div)	0.38
Change of divergence, relative to the grid average	ΔARR = 0.31 + 0.29 (Div)	0.37
Divergence of moisture flux	ΔARR = 0.32 + 0.02 (DivMF)	0.29
Divergence	ΔARR = 0.31 + 0.16 (Div)	0.26
Divergence of moisture flux, relative to the grid average	ΔARR = 0.30 + 0.01 (DivMF)	0.26

* Units of ΔARR are mm $h^{-1}(24\ min)^{-1}$, those of Div and DivMF $10^{-5}\ s^{-1}$.

age. But, the banded echoes had a much more substantial number of significant correlations. The larger echoes, as they did with the maximum intensity, generally correlated more than twice as well as the smaller ones. Again, smaller echoes did have a few significant correlations, all of which were with surface parameters which correlated poorly with the larger echoes. Those categories were the changes of divergence and divergence of moisture flux, and those parameters relative to the grid averages. The correlation coefficients ranged from 0.40 to 0.48, where the critical correlation coefficient for significance was 0.33.

c. *Change of average rainfall rate*

The relationship of the change of average rainfall rate to the surface parameters is not nearly as consistent as the two preceding relationships, but it is considered worth mentioning. The correlation coefficients and regression equations are listed in Table 8. Contrary to the maximum intensity and average rainfall rate results, the change of the average rainfall rate correlated quite poorly to any of the relative vorticity parameters. Apparently, the relative vorticity best relates to the actual values of these echo parameters at specific times, while fields such as the change of the divergence of moisture flux better relate to the changes of echo parameters in time. The change of the divergence fields did give better relationships with the average rainfall rate than the divergence fields at either the time of the echo or the previous hour. This shows that as an echo moves into an area, the more that echo is increasing its average rainfall rate, the more divergent the wind field becomes. This seems consistent considering the stronger downdrafts which would be associated with the more intense rainfall.

A scatter diagram of the change of divergence of moisture flux over the 1 h period preceding the time of the echo versus the change of the average

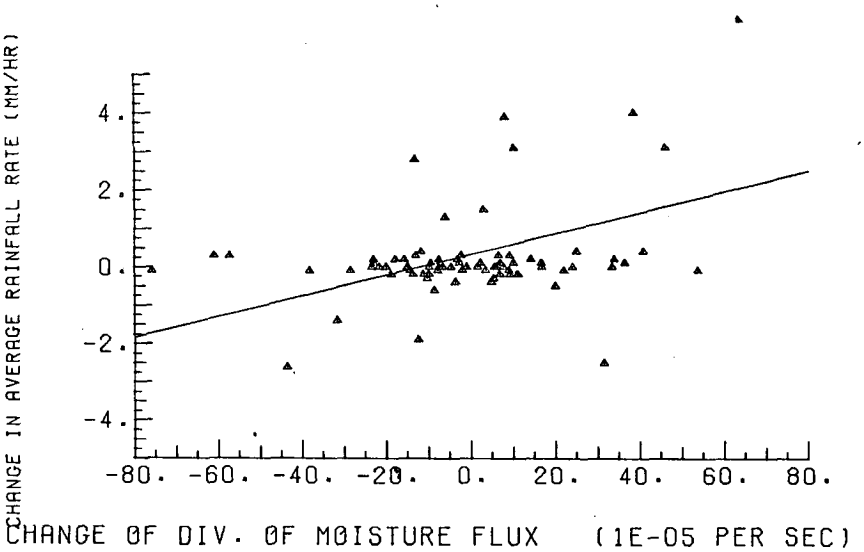

FIG. 9. Scatter diagram of the 24 min change of average rainfall rate versus the 1 h change of divergence of moisture flux.

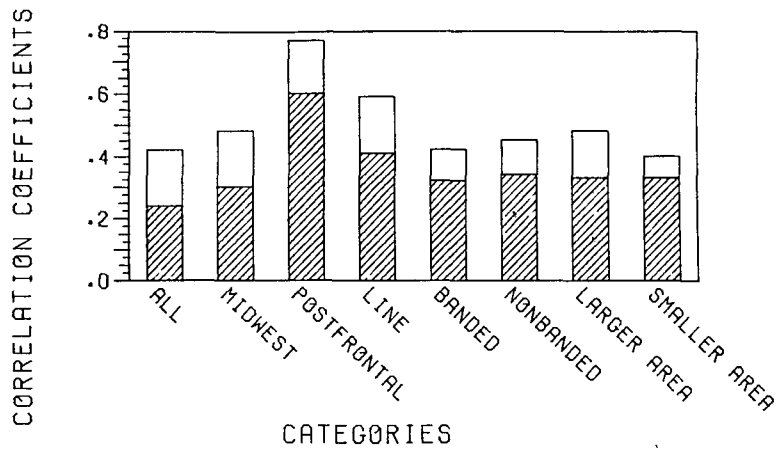

FIG. 10. Distribution of correlation coefficients for the relationship shown in Fig. 9, by echo category. See Fig. 6.

rainfall rate during the 24 min period the echo was observed is presented as Fig. 9. As can be seen, this relationship is not described very well by the linear regression equation. The change of rainfall rate values tend to be concentrated around zero, while the divergence values show much better distribution.

The distribution of significant correlation coefficients by each category is shown in Fig. 10. The reason for the significant correlations in the midwestern and postfrontal echo categories as opposed to none in their corresponding categories remains a mystery. The echoes which are part of lines continue to show up occasionally with significant correlations. In contrast to the previous echo parameters, there were no substantial differences between the banded and nonbanded categories and the larger and smaller echo categories for the change of the average rainfall rate.

6. Conclusions and recommendations

The use of a computer-interactive graphic display system (McIDAS) in this study provided for a very fast and efficient method of analysis of the digitized radar data. This method is recommended for small to medium size studies, where a fast method of analysis is desired, but complete control of the data is to be retained. However, for larger studies where more than a couple hundred echoes are to be used, the completely automated methods would probably be preferable due to the overwhelming costs involved in time and money. This type of system would be ideal in terms of operational use where a man-machine mix is desired.

The maximum intensity and average rainfall rate of the echoes showed significant correlation with many of the surface parameters tested, particularly the relative vorticity. These correlations were improved by using values of the surface fields for the area covered by the echo, 1 h before it arrived there; and also by finding the value relative to the grid average. Banded echoes had much better correlations than nonbanded ones, with the same true for large echoes compared with small echoes (<750 km^2). The divergence of moisture flux correlated better than the divergence of the wind alone. While the change of average rainfall rate for the echoes did not give as good relationships as the other two radar parameters, some significant correlations were found, particularly with the change of divergence of moisture flux.

When applying the relationships discussed in this study to operational forecasting, caution must be exercised. Since there were no dry cases (no radar echoes) used in the analysis, the relationships presented apply only in cases where an echo already exists. If a forecast is made of where the echo will be in 1 h, the relationships involving the time lag can be applied directly to predict the intensity characteristics.

The relationships presented here did not show high correlations, in that at best only 25% of the variance has been accounted for. One of the reasons the relative position of radar echoes and surface kinematic features is so variable may be the fact that the echoes sampled were at different stages of development. A storm in its early stages would have a different relationship to the surface fields than mature storms. These factors must be taken into account. Thus, multiple regression involving the past history of the echo would most likely give much better results. A larger data sample would be needed to give more definite regression equations for modeling use. Finally, since the results of this study point strongly to the idea that there is a time lag between occurrences on the surface and what

happens in the clouds, studies should be made to examine this in more detail.

There are many effects which disturb the surface wind field, making it very difficult to generate accurate divergence or vorticity fields. One solution which would give better results would be to use the wind field at or slightly below cloud level. The present radiosonde network is not of sufficient density to provide such data, and probably never will be. One possible source of such data is from satellites. Currently, winds are being generated from satellite picture loops. If enough clouds could be tracked in the area of the precipitation, detailed wind fields at the cloud level could be used for generating divergence and vorticity fields. There are undoubtedly many problems involved, but it seems to be worth pursuing. Another source would be by a dense network of remote sounding devices such as lidar.

In any case, it appears possible to make reasonable forecasts of the movement of radar echoes and forecast their intensity based on synoptic-scale parameters and the echoes' past histories. In future years, when fine-resolution digitized radar is installed nationwide, endless amounts of data should be available for massive statistical analyses.

Acknowledgments. The first author is deeply indebted to the National Weather Service for providing one year of graduate study at the University of Wisconsin, as well as to the many people who assisted in completing the research. We are grateful to Professors Eberhard W. Wahl and Gerald F. Herman for their constructive criticism. Paul Wofsy and Nancy Nagle of the Office of Technical Services, National Weather Service, and Horace Hudson of the National Severe Storms Forecast Center helped by furnishing data. Donald Wylie, John Stout and Gary Chatters of the Space Science and Engineering Center at the University of Wisconsin, as well as Thomas Whittaker and Peter Guetter of the University, gave much needed computer programming assistance. Robert Elvander and Robert Saffle of the Systems Development Office, National Weather Service, were helpful consultants in the use of digitized radar data. We also want to thank Thomas Koehler for his assistance in the research. The constructive comments from the anonymous reviewers were most appreciated. Funding for this research came from the National Weather Service and National Science Foundation Grant ATM77-20231.

REFERENCES

Austin, J. M., and R. H. Blackmer, Jr., 1956: The variability of cold front precipitation. *Bull. Amer. Meteor. Soc.*, **37,** 447–453.

Boucher, R. J., and R. Wexler, 1961: The motion and predictability of precipitation lines. *J. Meteor.*, **18,** 160–171.

Byers, H. R., and L. J. Braham, 1949: *The Thunderstorm.* U.S. Govt. Printing Office, Washington, DC, 287 pp.

Chatters, G. C., and V. E. Suomi, 1975: The applications of McIDAS. *IEEE Trans. Geosci. Electron.*, **GE-13,** 137–146.

Cox, M. K., 1959: The distribution and variability of cold-front precipitation. *Bull. Amer. Meteor. Soc.*, **40,** 477–480.

Cruz, L. A., 1973: Venezuelan rainstorms as seen by radar. *J. Appl. Meteor.*, **12,** 119–126.

Elvander, R. C., 1976: An evaluation of the relative performance of three weather radar echo forecasting techniques. *Preprints 17th Conf. Radar Meteor.*, Seattle, Amer. Meteor. Soc., 526–532.

Harper, W. G., and J. G. D. Beimers, 1958: The movement of precipitation belts as observed by radar. *Quart. J. Roy. Meteor. Soc.*, **84,** 242–249.

McGrew, R. G., 1972: Project D/RADEX (Digitized Radar Experiments). *Preprints 15th Radar Meteor. Conf.*, Urbana, Amer. Meteor. Soc., 101–106.

Mielke, K. B., and D. D. Houghton, 1977: An analysis of radar echo systems for the upper midwestern United States. *J. Appl. Meteor.*, **16,** 833–843.

Myers, J. N., 1964: Preliminary radar climatology of central Pennsylvania. *J. Appl. Meteor.*, **3,** 421–429.

Newton, C. W., and J. C. Fankhauser, 1964: On the movements of convective storms, with emphasis on size discrimination in relation to water-budget requirements. *J. Appl. Meteor.*, **3,** 651–668.

Pielke, R. A., and W. R. Cotton, 1977: A mesoscale analysis over south Florida for a high rainfall event. *Mon. Wea. Rev.*, **105,** 342–362.

Saffle, R. E., 1976: D/RADEX products and field operation. *Preprints 17th Conf. Radar Meteor.*, Seattle, Amer. Meteor. Soc., 555–559.

——, and D. R. Greene, 1978: The role of radar in the flash flood watch warning system: Johnstown reexamined. *Preprints 18th Conf. Radar Meteor.*, Atlanta, Amer. Meteor. Soc., 468–473.

Smith, E. A., 1975: The McIDAS system. *IEEE Trans. Geosci. Electron.*, **GE-13,** 123–136.

Ulanski, S. L., and M. Garstang, 1978: The role of surface divergence and vorticity in the life cycle of convective rainfall. Part 1: Observation and analysis. *J. Atmos. Sci.*, **35,** 1047–1062.

Whittaker, T. M., 1976: A simplified grid interpolation scheme for use in atmospheric budget studies. M.S. thesis, University of Wisconsin, 42 pp.

——, and R. A. Petersen, 1977: Objective cross-sectional analyses incorporating thermal enhancement of the observed winds. *Mon. Wea. Rev.*, **105,** 147–153.